

This Page Is Inserted by IFW Operations
and is not a part of the Official Record

BEST AVAILABLE IMAGES

Defective images within this document are accurate representations of the original documents submitted by the applicant.

Defects in the images may include (but are not limited to):

- BLACK BORDERS
- TEXT CUT OFF AT TOP, BOTTOM OR SIDES
- FADED TEXT
- ILLEGIBLE TEXT
- SKEWED/SLANTED IMAGES
- COLORED PHOTOS
- BLACK OR VERY BLACK AND WHITE DARK PHOTOS
- GRAY SCALE DOCUMENTS

IMAGES ARE BEST AVAILABLE COPY.

**As rescanning documents *will not* correct images,
please do not report the images to the
Image Problem Mailbox.**

Antisense *MBD2* gene therapy inhibits tumorigenesis

Andrew Slack¹

Veronica Bovenzi¹

Pascal Bigey²

M. A. Ivanov²

Shyam Ramchandani¹

Sanjoy Bhattacharya¹

Benjamin tenOever¹

B. Lamrihi²

Daniel Scherman²

Moshe Szyf^{1*}

¹Department of Pharmacology and Therapeutics, McGill University, 3655 Drummond Street, Montreal, PQ H3G 1Y6 Canada

²UMR 7001 CNRS-ENSCP-Aventis Gencell, Paris, France

*Correspondence to: Dr Moshe Szyf, McGill University, Department of Pharmacology and Therapeutics, 3655 Drummond Street, Montreal, PQ H3G 1Y6 Canada.
E-mail: mszyf@pharma.mcgill.ca

Received: 18 June 2001

Revised: 2 April 2002

Accepted: 2 April 2002

Abstract

Background Aberration in the pattern of DNA methylation is one of the hallmarks of cancer. We present data suggesting that dysregulation of *MBD2*, a recently characterized member of a novel family of methylated DNA binding proteins, is involved in tumorigenesis. Two functions were ascribed to *MBD2*, DNA demethylase activity and repression of methylated genes.

Methods Multiple antisense expression and delivery systems, transfection, electrotransfer and adenoviral were employed to demonstrate that *MBD2* is essential in tumorigenesis, both *ex vivo* and *in vivo*.

Results Inhibition of *MBD2* by antisense expression resulted in inhibition of anchorage-independent growth of antisense transfected cancer cells or cells infected with an adenoviral vector expressing *MBD2* antisense. Xenograft tumors treated with an adenoviral vector expressing *MBD2* antisense or xenografts treated with electrotransferred plasmids expressing *MBD2* antisense showed reduced growth.

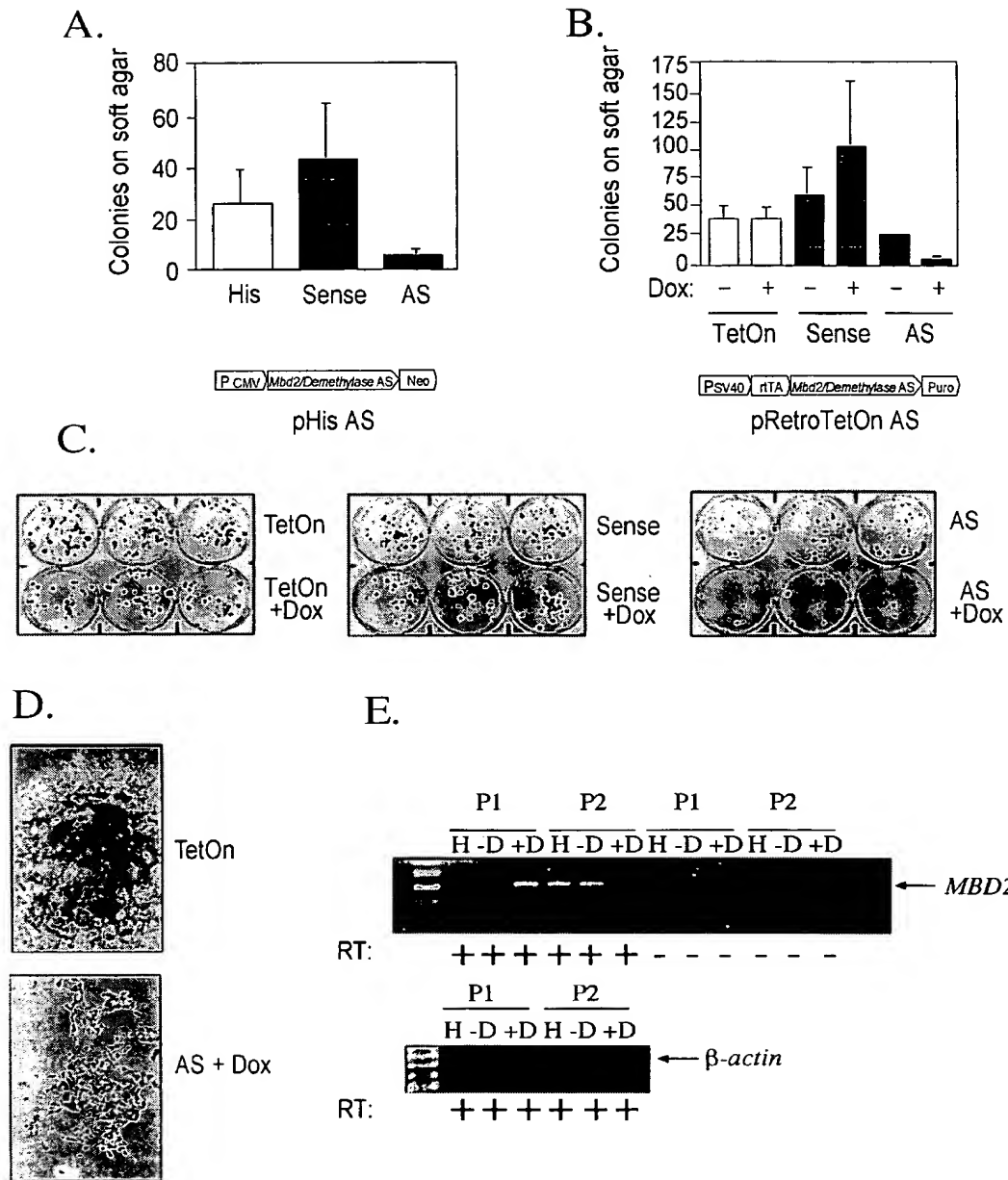
Conclusions These results support the hypothesis that one or both of the functions described for *MBD2* are critical in tumorigenesis and that *MBD2* is a potential anticancer target. Copyright © 2002 John Wiley & Sons, Ltd.

Keywords adenoviral vectors; DNA methylation; demethylase; methylated DNA binding proteins; tumorigenesis; antisense

Introduction

DNA methylation is an important epigenetic mechanism regulating gene expression [1–4]. One of the hallmarks of cancer cells is an aberrant methylation pattern [5]. Two contradictory changes in the methylation pattern have been previously documented, hypermethylation of selected genes [6] and global hypomethylation [7]. It is currently unclear what mechanisms are responsible for these changes. It is possible that these methylation changes are a consequence of deregulation of expression of the different components of the DNA methylation machinery [8]. The DNA methylation machinery is composed of DNA methyltransferases [9], demethylases [10–12] and methylated DNA binding proteins (MBDs) that interpret the DNA methylation signal [13]. A number of observations have supported the hypothesis that deregulation of the maintenance DNA methyltransferase *DNMT1* plays an important role in tumorigenesis [14–16]. An important question is whether other components of the DNA methylation machinery are also critical for cellular transformation [8,17].

Hypermethylation of tumor suppressor genes has been proposed to serve as a mechanism for silencing critical genes that are inhibitory of different steps



in tumorigenesis, thus promoting this process [18]. Methylated cytosines are specifically recognized by MBDs [13,19–21], which associate with co-repressors such as Sin3A, recruit histone deacetylases to methylated genes [22–26] and are found in known transcriptional repression complexes such as Mi2 [27].

MeCp2, which is the best characterized member of the family, is probably not very important in silencing genes during transformation since it is not expressed in cancer cells [20]. Other candidate proteins must be involved. A newly characterized methylated DNA binding protein, MBD2/demethylase, is an interesting candidate for the following reasons. First, the cDNA was cloned from a cancer cell line cDNA library [28] and is expressed in multiple tumors and cell lines [29]. The expression of the mRNA is upregulated in some cancers such as ovarian cancer [30] and downregulated in others such as colorectal cancer [31] and hepatocellular carcinoma [32]. It is unclear yet whether the protein levels exhibit a similar pattern. In ovarian cancers the expression of *MBD2/demethylase* correlates with demethylation of CpG sites in the promoter region of *c-erbB-2* and *survivin* [30], supporting its role in demethylation of tumor-related genes. Second, the protein is involved in gene suppression by a mechanism similar to the one shown for MeCp2 [24,27]. We have also reported that it exhibits a demethylase activity [28], but this has been disputed by a number of other groups [24]. These discrepancies remain to be resolved. Two isoforms of MBD2 have been described, MBD2a and MBD2b, using different initiation methionine. MBD2a is the longer isoform with 411 aa, while MBD2b is truncated on the N-terminus. Both can be expressed as mature proteins in HeLa cells [24]. The Mbd2b isoform was shown to possess demethylase activity [28].

MBD2 could be part of the machinery involved in mediating or interpreting the two contradictory changes associated with the DNA methylation pattern in cancer cells, i.e. hypermethylation and hypomethylation. In this

study we test the hypothesis that antisense *MBD2* gene therapy inhibits tumorigenesis.

Materials and methods

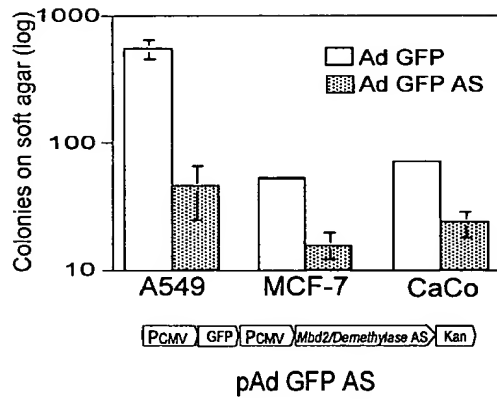
Strand-specific Northern blot and RT-PCR

To detect changes in *MBD2* mRNA levels following antisense treatment, RNA prepared from treated cells was fractionated and Northern blotted onto Hybond N+ membranes using standard procedures [33]. The membrane was hybridized with a ^{32}P -labeled *MBD2* antisense strand-specific riboprobe that was generated by *in vitro* transcription with T7 RNA polymerase (Roche) of Bluescript SK plasmid containing *MBD2b* cDNA [28] in the antisense orientation to the T7 promoter. The riboprobe (2×10^6 cpm) was added to 20 ml of ZipHyb Northern Max Plus hybridization buffer (Ambion) and the membrane was hybridized for 15 h at 68°C. Following stringent washing at 72°C, the membrane was exposed to autoradiography. To normalize for total RNA loading, the Northern blot was then stripped and hybridized with ^{32}P -labeled oligonucleotide probe for 18s rRNA as previously described [34].

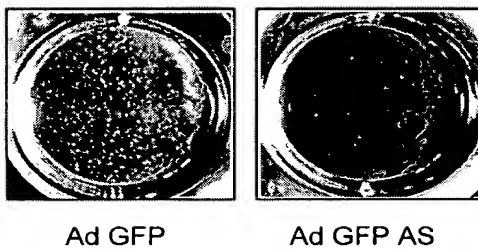
Strand-specific RT-PCR was used to verify expression of the antisense expression vectors in cells and *in vivo*. RNA (1 µg) prepared from either cells or tumor tissue was treated with 16U DNase I from the DNA-free kit (Ambion) for 3 h at 37°C to eliminate contaminating genomic DNA. The DNase I was inactivated with the DNase inactivation reagent, and the RNA was extracted with phenol/chloroform. The DNA-free RNA was then reverse-transcribed with 200U Mo-MuLV reverse transcriptase (MBI) using either specific sense P1 (5'ctggcaagagcgat gtc3') or antisense P2 (5'agtctggtttaccctattttg3') primers homologous to *MBD2*. The reverse-transcribed reaction (1 µl) was digested with DNase-free RNase in 10 µl. Then, 1 µl of this digest was amplified with the above-described

Figure 1. Antisense inhibition of *MBD2/Demethylase* inhibits anchorage-independent growth of a transformed human kidney cell line, HEK 293. (A) HEK 293 cells were transiently transfected with 10 µg pHis control (His), pHis sense (Sense) or pHis antisense (AS) *MBD2* plasmids and plated on soft agar 48 h later for determination of anchorage-independent growth, as described in Materials and Methods. The results represent an average of triplicate determinations \pm SD. Lower panel shows a schematic with important features of the pHis *MBD2* antisense vector (pHis AS) including the CMV promoter, P CMV; *MBD2/Demethylase* antisense insert; Neomycin selection gene, Neo. (B) HEK 293 cells were transiently transfected with 10 µg pRetro-TetOn control (TetOn), pRetroTetOn sense (Sense) or pRetroTetOn antisense (AS) *MBD2* plasmids, treated with and without 10 µg/ml doxycycline (Dox) and plated on soft agar 48 h later for determination of anchorage-independent growth. Lower panel shows a schematic with important features of the pRetro TetOn *MBD2* antisense vector (pRetro TetOn AS) including the SV40 promoter, P SV40; doxycycline-responsive reverse tetracycline activator element, rtTA; *MBD2* antisense insert; puromycin selection gene, Puro. (C) Cells treated as in (B) were also plated on regular tissue culture dishes, then stained and photographed after 14 days. Treatments were performed in triplicate as shown. (D) Enlarged images of colonies growing on tissue culture dish show the different morphology of control transfectants (TetOn) and *MBD2* antisense expressing transfectants (AS+Dox). (E) Strand-specific RT-PCR was used to verify that an *MBD2* antisense message was transcribed in the pRetroTetOn antisense clone (AS) induced with doxycycline (Dox) 10 µg/ml but not in the non-induced clones or in control cells. H, untransfected HEK cells; -D, pRetro TetOn AS no Dox; +D, pRetro TetOn AS plus Dox; P1, *MBD2*-specific sense primer used for reverse transcription; P2, *MBD2*-specific antisense primer used for reverse transcription. To confirm the specificity of reverse transcription from the strand-specific primer we subjected the reverse-transcribed cDNA to PCR amplification with primers for an abundant housekeeping gene, β -actin as indicated in the figure and demonstrated that there is no signal. Control reactions were performed in the absence of reverse transcriptase to demonstrate that residual contaminating DNA is not present in our RNA preparations

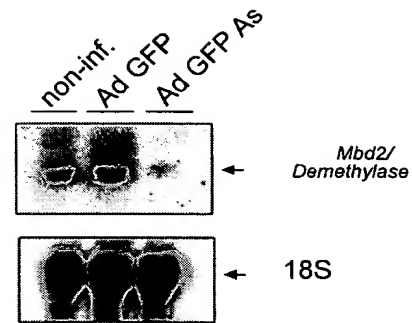
A.



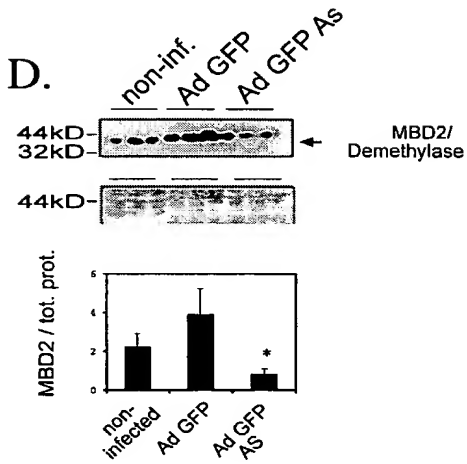
B.



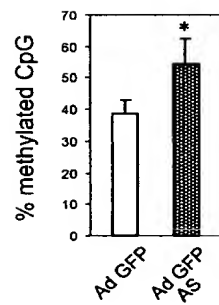
C.



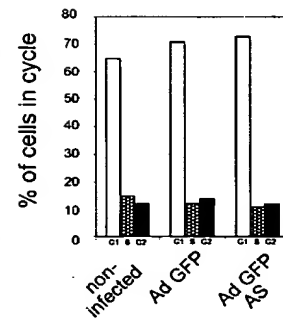
D.



E.



F.



primers using Taq polymerase (MBI) for 30 cycles of: 95°C, 30 s; 53°C, 30 s; 72°C, 1 min.

Western blots

To determine the levels of expression of MBD2 protein in treated A549 cells, 50 µg of total protein extracts were subjected to a Western blot analysis using standard procedures [33] and were reacted with a monoclonal antibody generated against the methylated DNA binding domain of MBD2 (Imgenex, San Diego, CA, USA). The total proteins transferred onto the nitrocellulose membrane were visualized using a BLOT-FastStain kit (Chemicon International).

Expression constructs

The human *MBD2* cDNA was cloned from a HeLa cell cDNA library in the TriplEx phage (Clontech) as described [28]. The *MBD2* insert was excised with NotI and subcloned into SK to generate riboprobes, the pcDNA 3.1 His expression vector (Invitrogen) and the doxycycline-inducible pRetroTetOn expression vector (Clontech) in both the sense and antisense orientations and the pAdTrack CMV adenoviral shuttle vector [35] in the antisense orientation. Recombinant pAd Easy adenoviral vectors were subsequently generated by recombination and high titer adenoviral stocks were purified as described [35,36].

Cell culture

HEK 293 human embryonal kidney cells (ATCC number CRL-1573), A549 non-small cell lung cancer cells (CCL-185), MCF-7 breast cancer cells (HTB-22), CaCo colon cancer cells and H1299 non-small cell lung cancer cells were cultured according to ATCC recommendations.

Tumorigenesis assays

For *ex vivo* soft agar analysis, A549 non-small cell lung cancer cells, MCF-7 breast cancer cells and CaCo colon cancer cells were plated at a density of 5.0×10^4 /well and infected the next day at a multiplicity of infection (MOI) of 100. For HEK 293 experiments, cells were plated at a density of 5.0×10^4 /well and transiently transfected with *MBD2* antisense in pHis or pRetro TetOn expression vectors the next day using the calcium phosphate precipitation method [33]. Forty-eight hours post-transfection, 3.0×10^3 viable cells were plated onto 0.33% agar with enriched media. Colonies were counted and photographed 14 days later as previously described [37]. For *in vivo* tumorigenesis studies, A549 and H1299 tumors were passaged in donor animals prior to implantation. A single tumor was sectioned and fragments were implanted sub-cutaneously in the right flank for all experiments. CD1 Swiss nu/nu athymic mice (6–8-week old; Charles River, Cambridge) were transplanted sub-cutaneously with 20 mm³ A549 tumor explants (in the case of adenoviral experiments) or H1299 tumor explants (in the case of the plasmid electrotransfer experiments). Treatment of tumors began when they reached a size of 30–100 mm³ approximately 1–2 weeks later. *In vivo* adenoviral infections were performed essentially as previously described [38]. Briefly, intratumoral injections were performed four times on alternate days with 5.0×10^9 pfu per injection with phosphate-buffered saline (PBS), control or antisense viruses. Tumor volume was then monitored for 4–5 weeks, after which the animals were sacrificed. Tumors were extracted, weights were determined and RNA was prepared for RT-PCR analysis. For electrotransfer *in vivo* experiments, intratumoral injections were performed 3 or 5 times every 2 to 5 days with either 50 µg plasmid (control or antisense) in 40 µl, or 150 mM NaCl using a Hamilton syringe and a 26-gauge needle. Both sides of the tumors were covered with conductive gel and placed between two flat parallel stainless steel electrodes 0.45 cm apart [39]. Twenty to

Figure 2. *MBD2* antisense expression inhibits anchorage-independent growth in a number of transformed cell lines, but does not arrest the cell cycle in normal diploid fibroblasts. (A) A549, MCF-7 and CaCo cells were infected at a MOI of 100 with control adenovirus (AdGFP) and antisense *MBD2* virus (AdGFP AS) and plated on soft agar 48 h later for determination of anchorage-independent growth as described. The results represent an average of triplicate determinations \pm SD. The statistical significances of the difference between the control and the antisense-infected cells were determined using a t-test; for the three cell lines used $p \leq 0.001$. Lower panel shows a schematic with important features of the pAd GFP *MBD2* antisense vector (pAd GFP AS) including the CMV promoter, P CMV; green fluorescent protein insert, GFP; *MBD2b/Demethylase* antisense insert; kanamycin selection gene, Kan. (B) Soft agar colonies of A549 cells treated with control virus (AdGFP) and antisense *MBD2* antisense virus (AdGFP AS) from the experiment described in (A) were photographed after 14 days. (C) RNA prepared from non-infected (non-inf.), control virus infected (AdGFP) and *MBD2* virus infected (AdGFP AS) A549 cells 48 h post-infection were Northern blotted and hybridized with an antisense *MBD2* riboprobe to quantify *MBD2* mRNA levels. The blot was stripped and rehybridized with an oligonucleotide homologous to 18S rRNA. (D) Cellular extracts prepared from identically treated A549 cells were subjected to a Western blot analysis using an MBD2-specific antibody as described in Materials and Methods. Each sample was loaded in triplicate and subjected to SDS-PAGE prior to Western blot analysis. The total proteins bound to the membrane were stained and quantification of the MBD2 relative to total protein is shown. An equal variance t-test analysis revealed significant differences between non-inf. and Ad GFP AS treated cells and between Ad GFP and Ad GFP AS treated cells ($p < 0.05$). (E) DNA prepared from control virus infected (AdGFP) and *MBD2* antisense infected (AdGFP AS) cells was subjected to a nearest neighbor analysis using ³²P-*adGTP*. The percentage of methylated cytosines in the dinucleotide sequence CpG was determined. The results are an average of three determinations \pm SD. A student t-test reveals a significant difference ($p < 0.05$) between GFP and the AS. (F) Fluorescence-activated cell sorting (FACS) analysis of non-infected (non-inf.), control virus infected (AdGFP) and *MBD2* antisense virus infected (AdGFP AS) MRHF cells. Percentage of cells in G1, S and G2 phases are plotted

thirty seconds after DNA injection, each tumor was subjected to 8 pulses of 20 ms duration at a voltage-to-distance ratio of 500 V/cm, delivered at the frequency of 1 Hz, using an electropulsator PS 15 (Jouan, St Herblain, France). Tumor volume was then monitored for 4–5 weeks.

Analysis of global DNA methylation status

Total genomic methylation status at CpG dinucleotide sequences was assayed as previously described using nearest neighbor analysis [28]. DNA (100 ng) is nicked with DNaseI (0.1 units) and then labeled with the single nucleotide ^{32}P - αdGTP using DNA polymerase1 (5 units). The relative frequency of the 5' neighbors of the labeled dGMP is determined by digesting the DNA with a 3' micrococcal mononuclease and separating the labeled mononucleotides by thin layer chromatography as described [28]. The intensity of the spots of methyl dCMP and dCMP is quantified by scanning densitometry. Each assay is performed in triplicate.

Results

Antisense *MBD2* expression inhibits anchorage-independent growth of E1A transformed human kidney embryonal cell line, HEK 293

We tested the hypothesis that *MBD2* is essential for the maintenance of the transformed state by measuring anchorage-independent growth on soft agar, which is one of the most reliable indicators of cell transformation *in vitro* [40], following its inhibition by antisense expression. We transiently transfected an expression vector expressing *MBD2b* in either the sense or the antisense orientation as well as an empty vector control into HEK 293 cells which are very efficiently transfected by this procedure (~70–100%). Transient transfection measures the immediate effects of *MBD2* inhibition on tumorigenesis and avoids the effects of integration sites and selection pressure. As shown in Figure 1A, transient transfection of *MBD2b* antisense results in a dramatic reduction in the capacity of the cells to grow in an anchorage-independent manner. *MBD2* and *MBD3* are homologous at the amino acids level but there is very poor homology at the nucleotide sequence, thus there is no concern that the *MBD2* antisense inhibits *MBD3* mRNA.

To verify that the inhibition of anchorage-independent growth is a consequence of *MBD2b* antisense expression and not the presence of the transfected plasmid DNA, we took advantage of the RetroTetOn doxycycline-inducible expression vector. As shown in Figures 1B and 1C, induced expression of *MBD2b* antisense results in almost complete inhibition of anchorage-independent growth of HEK293 cells. Whereas control transfectants

form multilayered colonies indicating loss of contact inhibition on regular tissue culture dishes, antisense expressing transfectants form a similar number of colonies but are flat and transparent indicating contact inhibited growth (Figure 1D). In Figure 1E, strand-specific PCR was performed to verify that a specific antisense message was expressed in the antisense clone induced with doxycycline, but not in the controls, and that *MBD2* mRNA is inhibited with the antisense.

In summary, *MBD2b* antisense expression reduces the capacity of transformed cells to grow in anchorage-independent or contact-inhibited conditions when plated at low density.

To test whether *MBD2* inhibition has a general effect on tumor cells or whether it is specific to HEK 293 cells, we generated an adenoviral-based antisense *MBD2b* vector AdGFP AS which was capable of efficiently infecting a variety of transformed cell lines. Infection of A549, MCF-7 and CaCo cell lines with AdGFP AS at a MOI of 100 for 48 h resulted in inhibition of soft agar colony growth in comparison to cells infected with the control AdGFP virus (Figure 2A). No significant effect on the viability of the cells or their number was observed during the infection period. Two typical wells are shown in Figure 2B.

As seen in Figures 2C and 2D, antisense expression results in reduction of both the *MBD2* mRNA and the *MBD2* protein, as determined by strand-specific Northern blot and Western blot analyses. The intensity of the signal obtained for *MBD2* was normalized to the signals obtained for total proteins transferred onto the nitrocellulose membrane. The quantification is presented in Figure 2D.

To test whether the expression of *MBD2b* antisense has an effect on the growth parameters of non-transformed cells, we infected MRHF cells, an immortalized diploid human fibroblast cell line, with either AdGFP or AdGFP AS for 48 h. Analysis of total DNA methylation showed a significant increase in methylated CpG in cells expressing AdGFP AS (Figure 2E). Analysis by fluorescence-activated cell sorting (FACS) revealed that expression of AdGFP AS had no effect on the cell cycle parameters of a non-transformed cell (Figure 2F). We did not detect a change in cell cycle parameters in any of the treated cancer cell lines either (data not shown).

MBD2b antisense expression reduces tumor growth *in vivo*

We utilized both plasmid and adenoviral-based gene delivery methods to test the hypothesis that *MBD2b* antisense expression inhibits tumorigenesis of human non-small cell lung carcinoma cells passaged in nude mice. Either pHis *MBD2b* antisense or pHis empty vector constructs were introduced into H1299 tumors *in vivo* by electrotransfer. *MBD2b* antisense treatment slows the progression of tumor growth relative to untreated controls and empty vector controls. Antisense treatment delayed by 9 days the time to reach an average size of 1000 mm³ relative to empty vector control and by

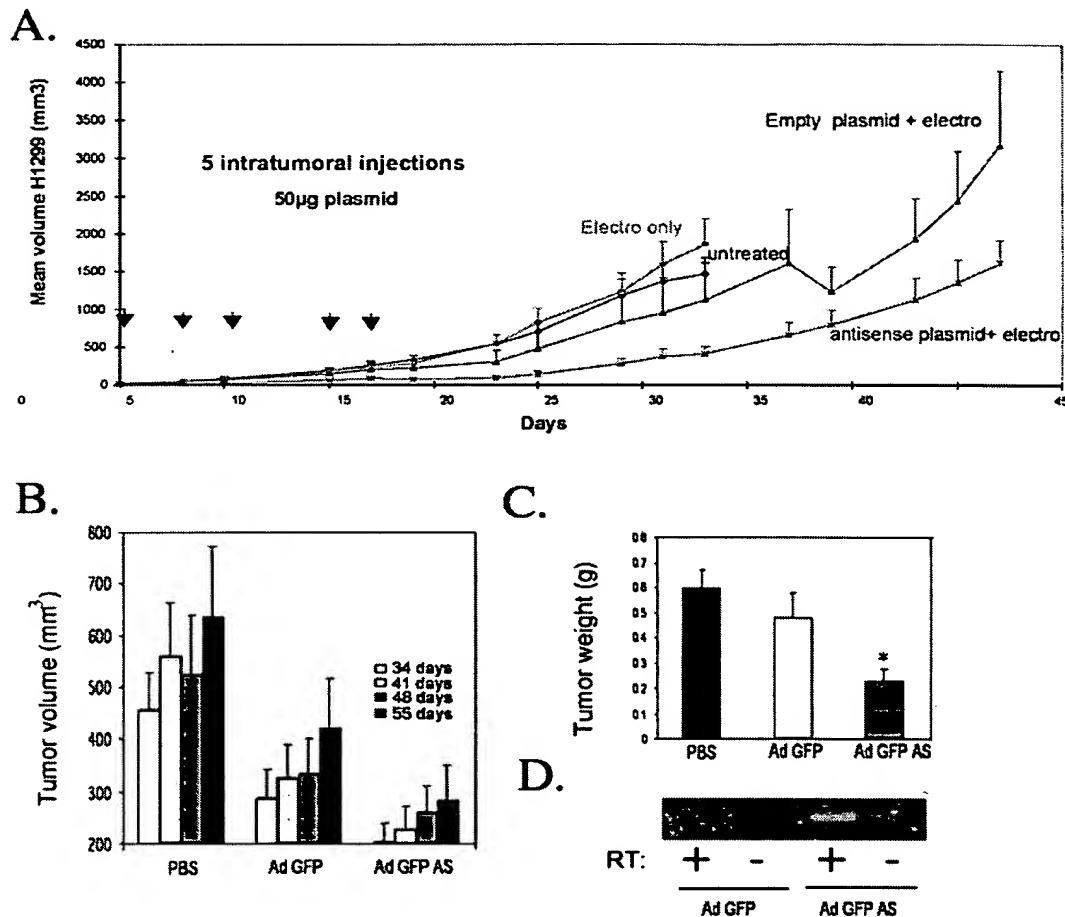


Figure 3. Antisense expression of *MBD2* results in a reduction in tumor growth *in vivo*. (A) Electrotransfer of 50 µg of either His vector, His *MBD2* AS or electrotransfer procedure alone was performed on xenograft H1299 tumors in nude mice. Volumes (mm³) are plotted against time over 42 days post-implantation. 10 animals per condition were used and results are plotted as means ± SD. Latency to reach a tumor volume of 1000 mm³ was found to be significantly different between the antisense group and untreated or mock electroporated ($p < 0.0001$ by either student t-test or Log-Rank Kaplan Meier) groups but not between the empty plasmid and the untreated groups. Detailed statistical analysis of this experiment is presented in Table 1. (B) Xenograft A549 tumors were infected with either Ad FP or Ad GFP AS or injected with PBS. Volumes were plotted for various days (34, 41, 48, 55 days) post-implantation. PBS (PBS), control adenovirus (Ad GFP) and antisense virus (Ad GFP AS) values are shown. Results are plotted as means ± SD. An equal variance t-test showed $p \leq 0.01$ for PBS against Ad GFP AS at days 34, 41, 48 and 55. The differences were significant for Ad GFP against Ad GFP AS at day 41 ($p = 0.05$) but less than significant for the other days ($p < 0.1$). (C) Tumor weights at the termination of the experiment were determined. PBS (PBS), control adenovirus (Ad GFP) and antisense virus (Ad GFP AS) values are shown. Results are plotted as means ± SD. An equal variance t-test reveals a significant difference ($p = 0.002$) between PBS-treated and antisense-treated tumors, between Ad GFP and Ad GFP AS treated ($p = 0.044$), but not between PBS-treated and Ad GFP-treated groups. (D) Strand-specific RT-PCR was used to verify that an *MBD2* antisense message was transcribed in the antisense-infected tumors (Ad GFP AS) *in vivo* but not in the control virus infected tumors (Ad GFP). Control reactions were performed without reverse transcriptase (RT).

15–18 days relative to untreated controls (Figure 3A). This experiment was performed twice more with similar results. Detailed statistical analysis of this experiment is presented in Table 1. Whereas the antisense treatment was statistically significant when compared with the PBS-treated control, the difference observed between the

antisense treated and empty plasmid treated did not attain statistical significance. Empty vector had an anti-tumorigenic effect in two separate experiments.

To validate these results, we used the adenoviral vectors described above to express *MBD2* antisense in human lung cancer carcinoma A549 tumors in nude mice.

Table 1. Statistical analysis of electrotransfer tumorigenesis experiment

	DAY 1000 mm ³ (median)*			
Group 1: untreated tumors	23.88			
Group 2: tumors treated with electrotransfer only	21.45			
Group 3: tumors treated with DNA demethylase antisense and electrotransfer	39.13			
Group 4: tumors treated with empty plasmid and electrotransfer	30.14			
Statistical comparison	Student t-test		Log-Rank	
DNA demethylase antisense electrotransfer versus untreated	Mean comparison $p=0.0001$	***	Kaplan Meier Risk to reach 1000 mm ³ tumor volume $p=0.0001$	***
DNA demethylase antisense electrotransfer versus electrotransfer only	$p=0.0003$	***	$p=0.0005$	***
empty plasmid electrotransfer versus untreated	$p=0.026$	NS	$p=0.0110$	*
empty plasmid electrotransfer versus electrotransfer only	$p=0.035$	NS	$p=0.0414$	*
DNA demethylase antisense electrotransfer versus empty plasmid electrotransfer	$p=0.10$	NS	$p=0.1353$	NS

*number of days to reach 1000 mm³ tumor volume.

***very significant.

Four consecutive intratumoral adenoviral injections (10 animals per group) totaling 1.0×10^{10} pfu of the Ad GFP AS vector resulted in a significant reduction ($p \leq 0.01$) in tumor growth relative to mice injected with the PBS control (Figure 3B). As observed with the electrotransfer experiment, we noticed an effect of the Ad GFP control vector alone on reduction of the tumor volume. Tumor weights determined at the conclusion of the experiment revealed a significant reduction of the mean tumor weight in animals treated with the Ad GFP AS vector as compared with PBS treatment and control GFP virus treatments (Figure 3C). As shown in Figure 3D, strand-specific RT-PCR revealed that antisense expression was detectable in a tumor infected *in vivo* with the Ad GFP AS virus but not in a tumor infected with control Ad GFP virus.

Discussion

This paper tests the hypothesis that a new member of the DNA methylation machinery, *MBD2*, plays a critical role in maintaining the transformed state of cancer cells and is a candidate target for inhibition by antisense gene therapy in cancer.

The results presented here are consistent with this hypothesis. First, we show that antisense-mediated inhibition of *MBD2* results in inhibition of colony formation in semisolid medium, a characteristic of transformed cells. Different methods of expression of antisense were utilized to rule out the possibility that the changes observed reflect some idiosyncratic property of the vector. Transient expression of antisense is sufficient to inhibit anchorage-independent growth, indicating that *MBD2* is required for maintenance of the transformed state and that its inhibition has immediate effects on cancer cell growth. In addition to this data, introduction of an adenoviral vector expressing *MBD2* antisense into human tumors passaged as xenografts in nude mice caused a significant reduction in tumor weight in comparison to animals treated with an adenoviral vector control, further

supporting the hypothesis that *MBD2* is required for maintenance of the transformed state. Nevertheless, further experiments are required to demonstrate the efficacy of *MBD2* antisense treatment *in vivo* because of the non-specific effect of vector DNA on tumor growth.

What is the mechanism by which inhibition of *MBD2* inhibits tumorigenesis? Since *MBD2* can repress methylated genes [24], and it has also been reported to bear a demethylase activity [28], it is possible that a number of genes are affected either way. Inhibition of *MBD2* might result in induction of tumor suppressor genes that are repressed by methylation, or silencing of some essential genes required for tumorigenesis by ectopic methylation. The data presented in Figure 2E suggests that inhibition of *MBD2* results in ectopic methylation. The identity of the genes that are either induced or suppressed by inhibition of *MBD2* will be determined in future experiments.

Whereas many questions remain unresolved, this paper shows that *MBD2* is a potential anticancer target. The fact that the cell cycle of normal cells is not affected by this treatment increases the attractiveness of this target. Further experiments will reveal which functions of this complex protein are essential for cellular transformation and tumorigenesis.

Acknowledgements

This study was supported by a grant from the National Cancer Institute of Canada to MS. We thank Ms. Johanne Theberge for her excellent assistance with the Western blot and nearest neighbor analyses.

References

1. Razin A, Szyf M. DNA methylation patterns. Formation and function. *Biochim Biophys Acta* 1984; 782: 331–342.
2. Razin A, Cedar H. Distribution of 5-methylcytosine in chromatin. *Proc Natl Acad Sci U S A* 1977; 74: 2725–2728.
3. Razin A, Riggs AD. DNA methylation and gene function. *Science* 1980; 210: 604–610.

4. Razin A. CpG methylation, chromatin structure and gene silencing: a three-way connection. *Embo J* 1998; 17: 4905–4908.
5. Baylin SB, Herman JG, Graff JR, et al. Alterations in DNA methylation: a fundamental aspect of neoplasia. *Adv Cancer Res* 1998; 72: 141–196.
6. Baylin SB. Abnormal regional hypermethylation in cancer cells. *AIDS Res Hum Retroviruses* 1992; 8: 811–820.
7. Feinberg AP, Vogelstein B. Hypomethylation distinguishes genes of some human cancers from their normal counterparts. *Nature* 1983; 301: 89–92.
8. Szyf M. DNA methylation properties: consequences for pharmacology. *Trends Pharmacol Sci* 1994; 15: 233–238.
9. Robertson KD, Uzvolgyi E, Liang G, et al. The human DNA methyltransferases (DNMTs) 1, 3a and 3b: coordinate mRNA expression in normal tissues and overexpression in tumors. *Nucleic Acids Res* 1999; 27: 2291–2298.
10. Weiss A, Cedar H. The role of DNA demethylation during development. *Genes Cells* 1997; 2: 481–486.
11. Jost JP, Siegmund M, Sun L, et al. Mechanisms of DNA demethylation in chicken embryos. Purification and properties of a 5-methylcytosine-DNA glycosylase. *J Biol Chem* 1995; 270: 9734–9739.
12. Ramchandani S, Bhattacharya SK, Cervoni N, et al. DNA methylation is a reversible biological signal [see comments]. *Proc Natl Acad Sci U S A* 1999; 96: 6107–6112.
13. Hendrich B, Bird A. Identification and characterization of a family of mammalian methyl-CpG binding proteins. *Mol Cell Biol* 1998; 18: 6538–6547.
14. MacLeod AR, Szyf M. Expression of antisense to DNA methyltransferase mRNA induces DNA demethylation and inhibits tumorigenesis. *J Biol Chem* 1995; 270: 8037–8043.
15. Laird PW, Jackson-Grusby L, Fazeli A, et al. Suppression of intestinal neoplasia by DNA hypomethylation. *Cell* 1995; 81: 197–205.
16. Ramchandani S, MacLeod AR, Pinard M, et al. Inhibition of tumorigenesis by a cytosine-DNA methyltransferase, antisense oligodeoxynucleotide. *Proc Natl Acad Sci U S A* 1997; 94: 684–689.
17. Szyf M. Targeting DNA methyltransferase in cancer. *Cancer Metastasis Rev* 1998; 17: 219–231.
18. Baylin SB, Herman JG. DNA hypermethylation in tumorigenesis: epigenetics joins genetics. *Trends Genet* 2000; 16: 168–174.
19. Meehan RR, Lewis JD, Bird AP. Characterization of MeCP2, a vertebrate DNA binding protein with affinity for methylated DNA. *Nucleic Acids Res* 1992; 20: 5085–5092.
20. Lewis JD, Meehan RR, Henzel WJ, et al. Purification, sequence, and cellular localization of a novel chromosomal protein that binds to methylated DNA. *Cell* 1992; 69: 905–914.
21. Cross SH, Meehan RR, Nan X, et al. A component of the transcriptional repressor MeCP1 shares a motif with DNA methyltransferase and HRX proteins. *Nat Genet* 1997; 16: 256–259.
22. Nan X, Ng HH, Johnson CA, et al. Transcriptional repression by the methyl-CpG-binding protein MeCP2 involves a histone deacetylase complex [see comments]. *Nature* 1998; 393: 386–389.
23. Jones PL, Veenstra GJ, Wade PA, et al. Methylated DNA and MeCP2 recruit histone deacetylase to repress transcription. *Nat Genet* 1998; 19: 187–191.
24. Ng HH, Zhang Y, Hendrich B, et al. MBD2 is a transcriptional repressor belonging to the MeCP1 histone deacetylase complex [see comments]. *Nat Genet* 1999; 23: 58–61.
25. Ng HH, Jeppesen P, Bird A. Active repression of methylated genes by the chromosomal protein MBD1. *Mol Cell Biol* 2000; 20: 1394–1406.
26. Boeke J, Ammerpohl O, Kegel S, et al. The minimal repression domain of MBD2b overlaps with the methyl-CpG binding domain and binds directly to Sin3A. *J Biol Chem* 2000; 275: 34963–34967.
27. Wade PA, Geggion A, Jones PL, et al. Mi-2 complex couples DNA methylation to chromatin remodelling and histone deacetylation [see comments]. *Nat Genet* 1999; 23: 62–66.
28. Bhattacharya SK, Ramchandani S, Cervoni N, et al. A mammalian protein with specific demethylase activity for mCpG DNA. *Nature* 1999; 397: 579–583.
29. Vilain A, Vogt N, Dutrillaux B, et al. DNA methylation and chromosome instability in breast cancer cell lines. *FEBS Lett* 1999; 460: 231–234.
30. Hattori M, Sakamoto H, Satoh K, et al. DNA demethylase is expressed in ovarian cancers and the expression correlates with demethylation of CpG sites in the promoter region of c-erbB-2 and surviving genes. *Cancer Lett* 2001; 169: 155–164.
31. Kanai Y, Ushijima S, Nakanishi Y, et al. Reduced mRNA expression of the DNA demethylase, MBD2, in human colorectal and stomach cancers. *Biochem Biophys Res Commun* 1999; 264: 962–966.
32. Saito KY, Sakamoto M, Saito H, Ishii H, Hirohashi S. Expression of mRNA for DNA methyltransferases and methyl-CpG-binding proteins and DNA methylation status on CpG islands and pericentromeric satellite regions during human hepatocarcinogenesis. *Hepatology* 2001; 33: 561–568.
33. Ausubel FM, Brent R, Kingston RE, et al. *Current Protocols in Molecular Biology*. John Wiley: New York, 1988.
34. Szyf M, Milstone DS, Schimmer BP, et al. cis-Modification of the steroid 21-hydroxylase gene prevents its expression in the Y1 mouse adrenocortical tumor cell line. *Mol Endocrinol* 1990; 4: 1144–1152.
35. He TC, Zhou S, da Costa LT, et al. A simplified system for generating recombinant adenoviruses. *Proc Natl Acad Sci U S A* 1998; 95: 2509–2514.
36. Knox JD, Araujo FD, Bigey P, et al. Inhibition of DNA methyltransferase inhibits DNA replication. *J Biol Chem* 2000; 275: 17986–17990.
37. Slack A, Cervoni N, Pinard M, et al. DNA methyltransferase is a downstream effector of cellular transformation triggered by simian virus 40 large T antigen. *J Biol Chem* 1999; 274: 10105–10112.
38. Mohan LS, Mohanam S, Kin Y, Sawaya R, Kyritsis AP, Nicolson GL, Rao JS. Downregulation of the urokinase-type plasminogen activator receptor through inhibition of translation by antisense oligonucleotide suppresses invasion of human glioblastoma cells. *Clin Exp Metastasis* 1999; 17: 617–621.
39. Mir OS. Mechanisms of electrochemotherapy. *Adv Drug Deliv Rev* 1999; 35: 107–118.
40. Freedman VH, Shin S. Cellular tumorigenicity in nude mice: correlation with cell growth and semi-solid medium. *Cell* 1974; 3: 355–359.